A 700-YEAR RECORD ON THE EFFECTS OF CLIMATE AND HUMAN IMPACT ON THE SOUTHERN CAPE COAST INFERRED FROM LAKE SEDIMENTS OF EILANDVLEI, WILDERNESS EMBAYMENT, SOUTH AFRICA

BASTIAN REINWARTH[1], SARAH FRANZ[1], JUSSI BAADE[1], TORSTEN HABERZETTL[1], THOMAS KASPER[1], GERHARD DAUT[1], JÖRG HELMSCHROT[2], KELLY L. KIRSTEN[3], LYNNE J. QUICK[3], MICHAEL E. MEADOWS[3] and ROLAND MÄUSBACHER[1]

[1]Physische Geographie, Institut für Geographie, Friedrich-Schiller-Universität Jena, Germany
[2]Biozentrum Klein Flottbek & Botanischer Garten, Universität Hamburg, Germany
[3]Department of Environmental & Geographical Science, University of Cape Town, South Africa

Reinwarth, B., Franz, S., Baade, J., Haberzettl, T., Kasper, T., Daut, G., Helmschrot, J., Kirsten, K.L., Quick, L.J., Meadows, M.E. and Mäusbacher, R., 2013. A 700-year record on the effects of climate and human impact on the southern Cape coast inferred from lake sediments of Eilandvlei, Wilderness Embayment, South Africa. *Geografiska Annaler: Series A, Physical Geography*, ••, ••–••. DOI: 10.1111/geoa.12015

ABSTRACT. The southern Cape coast, South Africa, is sensitive to climate fluctuations as it is influenced by different atmospheric and oceanic circulation systems. Palaeoecological evidence of Holocene climate variations in this region is presently limited. Here, we present a lake sediment record spanning approximately the last 670 years from Eilandvlei, a brackish coastal lake situated mid-way between Cape Town and Port Elizabeth. The results from geochemical and sedimentological analyses point to an increase in minerogenic sediment input from the catchment starting around AD 1400. Changes in the seasonal distribution of rainfall during the Little Ice Age may have altered river discharge and increased erosion rates and fluvial sediment transport in pre-colonial times. A rising mean lake level, possibly associated with an altered water balance or relative sea-level rise, may offer an explanation for the deposition of finer sediments. After AD 1450, reduced burial flux of elements associated with autochthonous sediment formation may have resulted from ecological changes in Eilandvlei. Enhanced sedimentation rates, increasing carbon, nitrogen, phosphorous and biogenic silica concentrations, as well as high concentrations of proxies for allochthonous sediment input (e.g. aluminium, titanium, zirconium) point to increasing sediment and nutrient flux into Eilandvlei from the late nineteenth century onwards. The most likely factor involved in these recent changes is land-use change and other forms of human impact.

Key words: South Africa, southern Cape, coastal lake, lake sediments, geochemistry, sedimentology, Little Ice Age, human impact

Introduction

South Africa is affected by tropical and subtropical, atmospheric and oceanic circulation systems leading to strong climatic and environmental gradients across the subcontinent (Scott and Lee-Thorp 2004). A long-term perspective on climatic oscillations and the effects of human interference are essential for environmental management and modelling of environmental and climate change scenarios. Unfortunately, climatic conditions often constrain the preservation of sedimentary records across much of the subcontinent, which partly explains the scarcity of palaeoenvironmental data from terrestrial archives (Chase and Meadows 2007).

Sediments of coastal lakes provide an opportunity for palaeoecological research and were previously used to reconstruct the evolution of South Africa's coastal environments and its driving forces, that is, climate, sea level fluctuations and human impact (Baxter and Meadows 1999; Gordon *et al*. 2012). Here, we present a sediment record from Eilandvlei, a coastal lake located in the Wilderness Embayment at the southern Cape coast (Fig. 1a). The sensitivity of this region to climate and sea-level change throughout the Holocene has already been demonstrated by studies of diatom, pollen and charcoal assemblages from Groenvlei (Martin 1959, 1968), palynological evidence from the Norga peat (Scholtz 1986) and the examination of large mammal remains at Nelson Bay Cave (Klein 1983; Fig. 1a). Detailed evidence for late Holocene temperature oscillations was inferred from a stalagmite record of the Cango Caves,

DOI:10.1111/geoa.12015

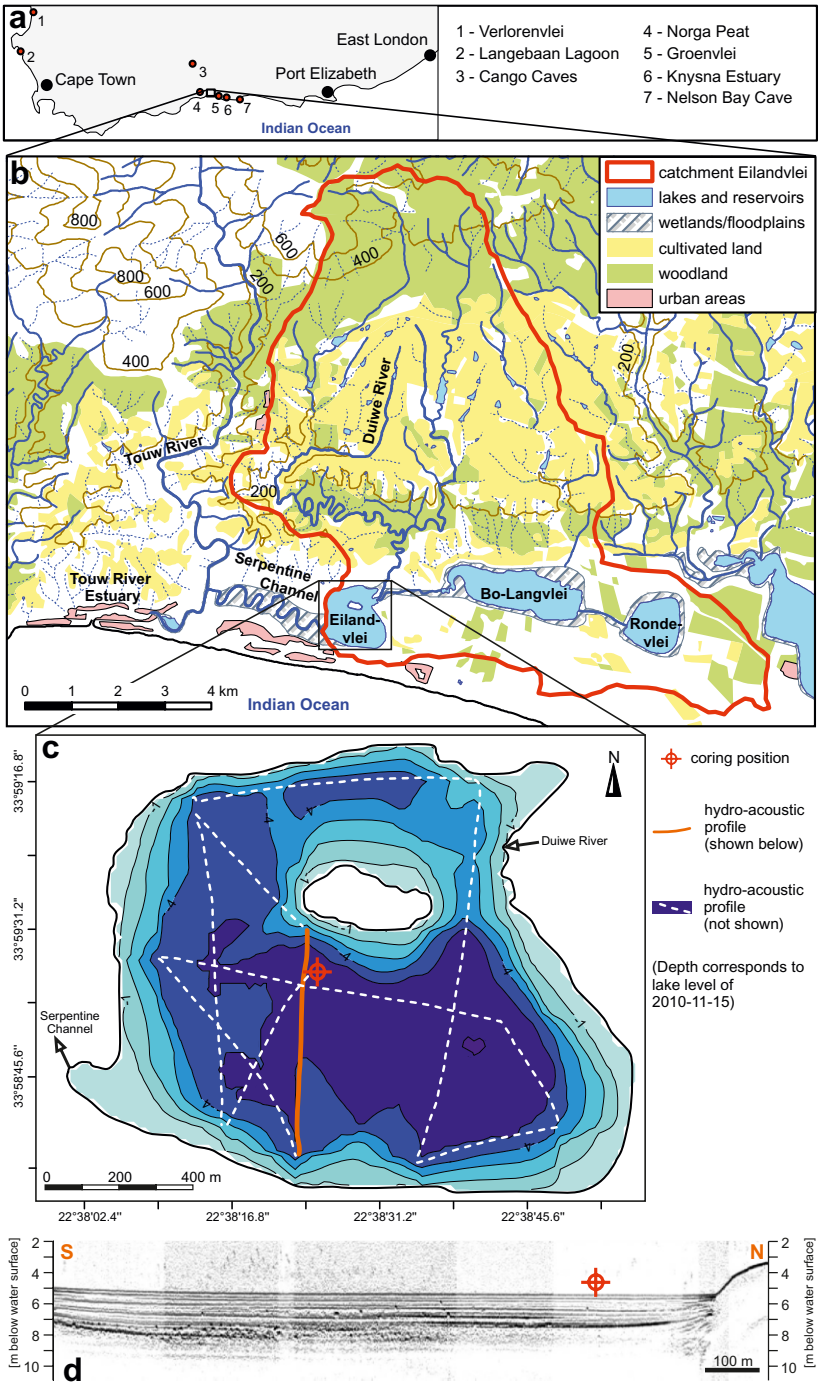

Fig. 1. Study site: (a) Location of the Wilderness Embayment and other sites mentioned in the text. (b) Land-use patterns in the catchment of Eilandvlei. Note several small farm ponds on the cultivated coastal platform (data source: Chief-Surveyor General 2007, http://csg.dla.gov.za/spatial.htm, 22-Jan-12; Jarvis, A., Reuter, H.I., Nelson, A. and Guevara, E., 2008, http://srtm.csi.cgiar.org (file: srtm_41_19.tif), 11-Jun-11). (c) Bathymetry of Eilandvlei with location of the coring site and (d) the hydro-acoustic profile (a sound velocity of 1492 m s^{-1} in the lake water was assumed).

~75 km north of the Wilderness region (Talma and Vogel 1992). However, high-resolution records providing insights into environmental dynamics during the late Holocene are currently not available.

The goal of this study is to contribute to a better understanding of late Holocene landscape dynamics in the Wilderness Lakes region. In tracing granulometric and geochemical parameters in a sediment core (65 cm) from Eilandvlei we aim to elucidate environmental dynamics in pre-colonial times (e.g. changes in sediment dynamics due to climate and/or sea level fluctuations); pre-colonial variations in the ecology of Eilandvlei; and the amplitude and effects of human impact following the arrival of European colonists.

Study area and site description

The Wilderness Embayment is characterized by a complex of Pleistocene dune cordons separating the Indian Ocean from a series of shallow brackish lakes (Bateman *et al*. 2011). The Wilderness Lakes, that is, Rondevlei, Bo-Langvlei and Eilandvlei, are surrounded by reed-covered wetlands and interconnected by channels that were artificially deepened after AD 1975 (Fig. 1b). Eilandvlei, that owes its name to an island situated in the middle of the lake, reaches ~6.5 m water depth (Weisser *et al*. 1992) and has a surface area of 1.48 km^2 (Watling 1977).

The lake is fed by the Duiwe River and drains via the Serpentine Channel and Touw River Estuary (Fig. 1c). The estuary mouth is frequently blocked by a sandbar (Russell 2003). In this situation, water is impounded depending on catchment discharge. Since the height difference between the water surface of the Touw River and Eilandvlei is normally < 0.3 m, water is ponded back which occasionally has resulted in slightly elevated lake levels (Coetzee 1983) and inundation of wide reed-covered areas during peak river discharge (Department of Water Affairs and Forestry 2012, unpublished data). The sandbar at the mouth of the Touw River Estuary is breached by overspilling water or by human intervention to prevent flooding of housing. When the estuary mouth is open, Eilandvlei is subject to a slight tidal influence and high spring tides may result in saline water entering the lake. These processes result in considerable temporal oscillation of hydrochemical parameters that affect biological activity within Eilandvlei (Coetzee 1983; Russell 2013).

The catchment is ~67 km^2 (Fig. 1b) and can be divided into the slopes of the Outeniqua Mountains (250–750 m a.s.l.), the coastal platform (150–250 m a.s.l.) and the coastal dune area (< 150 m a.s.l.). The geology is characterized by granites and metamorphic rocks (Potgieter 1949). A substantial portion of the coastal platform is covered by Pleistocene sand sheets (Illenberger 1996). Coastal dune cordons surrounding Eilandvlei have recently been stabilized to a large extent by introduced vegetation, although dune formation certainly proceeded throughout the late Holocene, especially at the seaward dune cordon (Bateman *et al*. 2011).

Mean annual precipitation of 600–1000 mm, almost uniformly distributed throughout the year, supports afrotemperate forests with intermediate fynbos shrubland patches (Allanson and Whitfield 1983). Fire incidence is an important control on the nature of local vegetation patterns (Geldenhuys 1994). Vegetation was markedly influenced by agriculture and forestry after the arrival of European colonists (Phillips 1931). Presently, agriculture is the predominant land use on the coastal platform, while afrotemperate forests, fynbos shrubland and plantation forestry cover the slopes of the Outeniqua Mountains (Fig. 1b). Protected fynbos communities and wetlands in the coastal dune area are intercalated with settlements.

Materials and methods

In November 2010, a sediment reconnaissance survey was carried out on three lakes of the Wilderness Embayment in order to find promising coring sites for a future in-depth coring campaign. Hydroacoustic data acquisition was conducted using a parametric sediment echo sounder (Innomar SES 96 light). Based on the results (Fig. 1d), a coring position ~160 m southeast of Eilandvlei's island (33° 59′ 35.04″ S; 22° 38′ 24.84″ E) was chosen. A sediment core labelled EV 10.1 with a length of 65 cm was recovered from ~5.5 m water depth using a modified ETH gravity corer (Kelts *et al*. 1986).

The sediment core was split and described lithologically using standard sketches and a Munsell Soil Colour Chart. Magnetic susceptibility measurements and X-ray fluorescence scanning was conducted in 2 mm steps as described in Kasper *et al*. (2012). For granulometric and geochemical analyses, the core was sub-sampled at 1 cm intervals with the exception of the uppermost 12 cm (for granulometric analysis, $N = 77$) and 22 cm (for geochemical analysis, $N = 87$) for which a 0.5 cm

Table 1. Mean concentrations (µg g^{-1}), mean absolute (µg g^{-1}) and mean relative (%) analytical errors (95% confidence interval, Student's *t* value = 4.03) calculated from triplicate measurements of samples taken from 3.25, 32.5 and 64.5 cm sediment depth and element-specific instrumental detection limits (µg g^{-1}).

Element	Al	B	Ba	Ca	Co	Cr	Cu	Fe	K	Mg	Mn	Na
Mean	54 000	54.7	128.5	3821	9.0	71.3	12.0	30 100	8280	5890	330	10 100
Abs.	1700	1.3	4.8	92	0.7	2.4	5.0	800	290	170	9	303
Rel.	3	2	4	2	8	3	41	3	4	3	3	3
Limits[1]	0.4	0.3	0.07	0.03	0.5	0.4	0.5	0.4	1.8	0.02	0.04	0.9

Element	Ni	P	Pb	S	Sr	Ti	Y	Zn	Zr	TOC*	TOC	TN
Mean	34.4	870	27.6	22 150	75.7	488	21.8	52.4	28.2	78 590	74 250	6819
Abs.	2.2	23	5.0	710	1.9	146	0.9	3.9	1.4	260	740	89
Rel.	6	3	18	3	3	30	4	7	5	< 1	1	1
Limits[1]	0.7	2.3	2.3	4.0	0.02	0.2	0.2	0.3	0.4	< 200	< 200	< 200

[1] Detection limits (3σ) were calculated from the weighed portions and information provided by the equipment manufacturers. According to DIN (2008), the determination limit is about three times the detection limit.

resolution was chosen. Samples were oven-dried (50°C for 72 h) to determine water content and bulk density. Grain sizes were measured with a Beckman Coulter laser diffraction particle size analyzer (LS 13320; Kasper *et al*. 2012*)*. Grain size fractions were calculated according to Ad-hoc AG Boden (2005); mean grain size was determined by the geometric method of moments as quoted by Blott and Pye (2001).

For geochemical analysis, samples were ground to < 40 µm. *Total carbon* (*TC*), *total nitrogen* (*TN*; $N = 87$) as well as *total organic carbon* (*TOC*) and *total inorganic carbon* (*TIC*, $N = 11$) were determined following Schneider *et al*. (2010) using a CNS element analyzer (Vario El). TOC and TIC concentrations were determined only for every eighth sample, since preliminary tests suggested negligible carbonate concentrations. The results confirmed that TOC accounts for 89–99% (mean 94%) of TC. Hence, the notation TOC* is used for TC contents that can be regarded as a good approximation for TOC concentrations and were determined with a higher resolution.

Element concentrations of 21 elements were determined ($N = 25$) by means of *inductively coupled plasma optical emission spectrometry* (*ICP-OES*; Varian Liberty 150). For this purpose, samples were digested with a microwave-based procedure using modified aqua regia [deionized water, HCl (30%, sp., Roth) and HNO_3 (30%, sp., Roth); ratio: 1:2:4]. Burial flux rates of elements were calculated according to Xu *et al*. (2009). Powder *X-ray diffraction* (*XRD*) measurements were carried out on samples from 0.75, 13.25, 26.5, 41.5 and 50.5 cm sediment depth using an AXS Bruker D8-Discover GADDS. *Biogenic silica* (*BSi*) concentrations ($N = 70$) were determined following the procedure of Ohlendorf and Sturm (2008) using a microwave-based NaOH digestion (2 h) and ICP-OES measurement. A correction factor of 2 to account for dissolving alumosilcates was chosen as this revealed consistent results in comparison to the method of DeMaster (1980).

Measurements on certified reference samples were carried out to ensure the reliability of the analytic results. Repeated measurement runs for the same sample imply an absolute instrumental error (95% confidence interval) of < 0.6%, < 1.3%, < 2.0% for clay, silt and sand, respectively, and < 0.5 µm for mean grain size. Table 1 summarizes absolute and relative measurement errors of element concentrations. Analytical errors of BSi concentrations ranged between < 0.1% and 0.35% SiO_2 eq. Statistical analyses of all data were carried out with the software R 2.15.0 (R Development Core Team, http://www.r-project.org, 2-Apr-12).

Due to the lack of macro remains, AMS radiocarbon dating (Beta Analytic, Inc., Miami, FL, USA) was carried out on the bulk organic fraction of six samples, each covering 1 cm of sediment depth. Conventional radiocarbon ages (± 1σ) were calibrated applying calibration curves for the southern hemisphere (McCormac *et al*. 2004; Manning and Melhuish 1994) using a set of linear interpolation methods implemented in Clam (Blaauw 2010) and the CALIBomb calibration data set (Reimer *et al*. 2004). Correction of possible reservoir effects was not carried out as a sample from 16.5 cm sediment depth contained post-modern carbon indicating a

reservoir effect of less than 60 years. Age determinations that indicated minor age reversals in the resulting age-depth model were treated as outliers. Younger ages were preferred in the model, because they appeared more plausible in the context of conceivable sediment remobilization and fluctuating minor reservoir effects.

Results

Sediment fabrics

Core EV 10.1 consists of dark greyish to greyish brown (Munsell Colour: 5–7.5 YR 3–5/2), thin bedded, clayey silt. The radiography reflects differences in bulk density and points to an undisturbed continuous sediment sequence (Fig. 2a) with beds varying in thickness from subcentimetre to centimetre scale. Only below 48 cm is some evidence for turbation visible. Diamagnetic effects of organic matter and a water content of 65–79% cause low magnetic susceptibility values (Dearing 1999) between –30 and 20×10^{-6} SI units. Based on changes in mean grain size, the sediment core was subdivided into three units, subsequently labelled Units I to III from the base of the core upwards (Fig. 2a–b). Moreover, Unit I was subdivided into Subunits Ia and Ib based on geochemical composition (e.g. TOC*, TN and BSi concentrations, TOC/TN ratio). A depth-constrained cluster analysis of granulometric and geochemical data using the CONISS algorithm (Grimm 1987) and standard scores supports this subdivision by objective criteria.

Chronology and sedimentation rates

According to a radiocarbon age obtained from a depth of 64.5 cm, the core base dates back to ~AD 1340 (AD 1280–1390; Table 2). The age-depth model (Fig. 3) shows variations in sedimentation rates on a decadal to centennial scale. Ages from 64.5, 48.5 and 32.5 cm point to mean sedimentation rates of ~0.2 cm yr^{-1} between AD 1340 and AD 1480. A distinct reduction of sedimentation rates by almost one order of magnitude to 0.03 cm yr^{-1} is apparent for the time span between AD 1480 and AD 1955. Highest sedimentation rates of ~0.3 cm yr^{-1} were calculated for the uppermost 16.5 cm sediment that post-date AD 1950.

Several chronological issues are worthy of further consideration. The reservoir effect of seawater along the southern Cape coast, although not extensively studied, may be of the order of 400–600 years (Sealy *et al*. 2006; Dewar *et al*. 2012). Fluctuating marine and terrestrial influences as well as inputs of carbonates derived from partially cemented dunes (Bateman *et al*. 2011) could evoke variable hardwater effects in Eilandvlei. In periods of increasing reservoir effects, radiocarbon ages would tend to overestimate sedimentation rates,

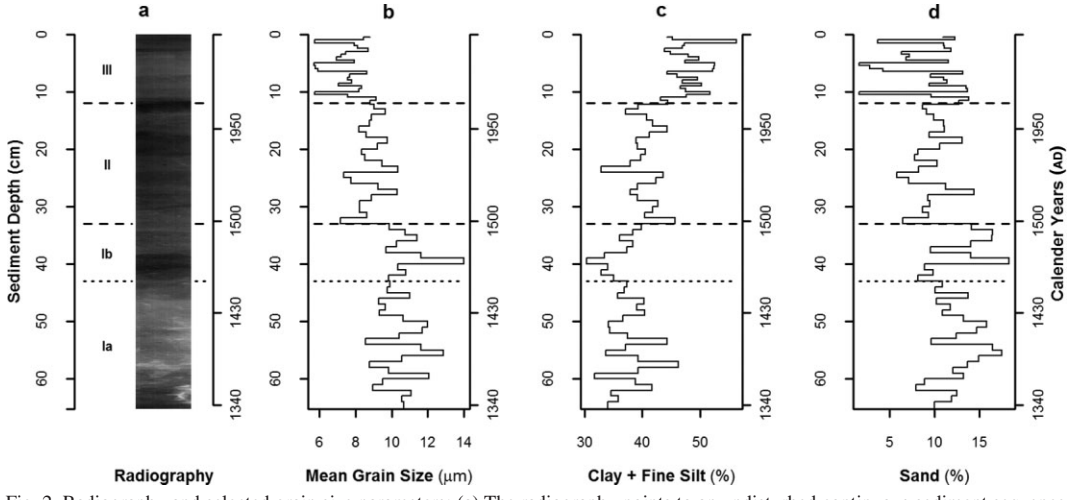

Fig. 2. Radiography and selected grain size parameters: (a) The radiography points to an undisturbed continuous sediment sequence with the exception of the core section below 48 cm sediment depth, where some signs of turbation are visible. (b) Mean grain size was calculated using the geometric method of moments as quoted by Blott and Pye (2001). (c) The sum of clay and fine silt and (d) sand percentage are given according to the German Soil classification (Ad-Hoc AG Boden 2005; see Table 3). Horizontal dashed lines show the borders of units and subunits.

Table 2. AMS radiocarbon datings from sediment core EV 10.1.

Lab. No.	Depth (cm)	$\delta^{13}C$[1] (‰)	Conventional ^{14}C age	Calibration curve	Calibrated ^{14}C age[2]
Beta-297677[3]	0–1	–25.5	30 ± 30 BP	Shcal04.14c	AD 1950 (1820–1955)[4]
Beta-297675	16–17	–24.0	105.4 ± 0.4 pMC[5]	Wellington	AD 1958[6] (1958–1959)
Beta-301558[3]	24–25	–24.3	500 ± 30 BP	Shcal04.14c	AD 1440 (1410–1475)
Beta-290786	32–33	–24.1	440 ± 30 BP	Shcal04.14c	AD 1480 (1435–1620)
Beta-297676	48–49	–25.1	530 ± 40 BP	Shcal04.14c	AD 1430 (1395–1460)
Beta-290787	64–65	–25.2	700 ± 40 BP	Shcal04.14c	AD 1340 (1285–1390)

[1] Ratios were calculated relative to the PDB-1 standard.
[2] Median age and 2σ range.
[3] Sample was treated as outlier due to a minor age reversal.
[4] AD 1955 represents the end of the Shcal04.14 calibration curve.
[5] pMC refers to percent modern carbon.
[6] Year of highest probability was used instead of median age.

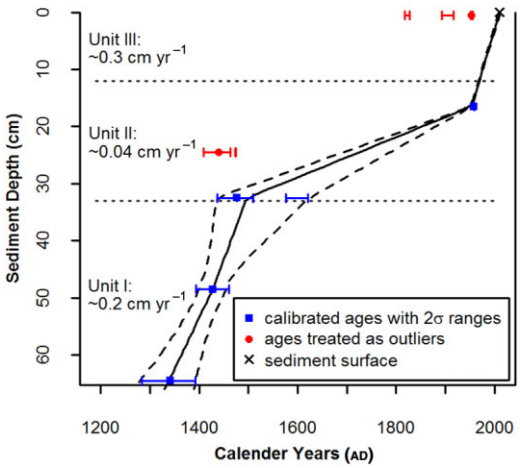

Fig. 3. Chronology of the sediment core EV 10.1. The age-depth model is based on best estimates (black solid line) which were derived using the Clam algorithm (Blaauw 2010). Dashed lines correspond to minimum and maximum age. Results obtained from samples taken in 24.5 and 0.5 cm sediment depth were not considered when setting up the chronology. Mean sedimentation rates of Units I, II and III correspond to best estimates.

while they underestimate them if enhanced freshwater influx leads to a long-term decrease of hardwater effects. Wave-induced resuspension within the lake in addition to reworking of sediment in the catchment, especially during flood events, might additionally contribute to the deposition of 'old carbon'. Radiocarbon dates indicating age reversals and the pre-nuclear bomb age of the surface sample is interpreted in this way. Stager *et al.* (2012) found an offset of 100–300 years between ages of organic bulk samples and plant remains in sediments of Verlorenvlei, a coastal lake of the western Cape coast (Fig. 1a). Therefore, it is conceivable, that apparent oscillations of mean sedimentation rates are partially influenced by dating uncertainties.

Lithostratigraphy

Three sedimentological units (Units I, II and III) were designated. The boundaries between the units are highlighted by changes in mean grain size, while an overall tendency of sediment fining towards the surface is recognizable (Figs 2b–d). In Unit I (65–33 cm; ~AD 1330–1490) mean grain size ranges between 8.5 and 14.0 µm. Based on the distinct decrease in TOC/TN ratios and BSi concentrations (Fig. 4) this unit was further divided into Subunits Ia (65–43 cm; ~AD 1330–AD 1450) and Ib (43–33 cm; ~AD 1450–AD 1490). TOC/TN ratios change from 14.2 to 12.5 (Fig. 4a) and BSi concentrations from above 4% SiO_2 eq. to below 3.4% SiO_2 eq. (Fig. 4b). In addition, Subunit Ia exhibits a rather low content of Al, Ti and Zr (i.e. proxies for minerogenic sediment input; Boës *et al.* 2011; Fig. 5), although Zr concentrations are slightly elevated below 56 cm (~AD 1390); Fe/S ratios are generally low. Concentrations of elements whose burial flux is likely to be controlled mainly by autochthonous processes and/or marine influences such as BSi, TOC*, TN, B, Ca and P (Figs 4b and 6) are high. Above 52 cm (~AD 1410), Al, Ti and Zr concentrations and Fe/S ratios increase continuously, while TOC*, TN, B, Ca and P contents are decreasing (Figs 5 and 6). In Subunit Ib, a core section with high bulk density is recognizable between 43 and 39 cm in the radiography (Fig. 2a), possibly related to layers with a higher sand content (Fig. 2d).

Unit II (33–12 cm; ~AD 1490–post AD 1950) is characterized by mean grain sizes ranging between 7.1 and 10.4 µm (Table 3). Fe/S ratios rise continuously; Zr and Al concentrations increase markedly at 20.25 cm (~AD 1850), and 14.25 cm (post AD 1950), respectively (Fig. 5), indicating a distinct increase of minerogenic sediment proportions. Despite decreasing concentrations of TOC* and P, TOC/TN ratios are fairly constant in the lower section of Unit II, but decrease steadily from 20.25 cm (~AD 1850) upwards (Figs 4a, 6a and 6d). Simultaneously TOC*, TN and P concentrations increase, a trend which is only interrupted by a 2 cm thick bed between 14.0 and 12.0 cm clearly visible in the radiography (Fig. 2a), that is characterized by very low BSi contents and lowered TOC* concentrations (Figs 4b and 6a).

Unit III (post AD 1950) exhibits lowest mean grain size ranging between 5.7 and 9.1 µm (Table 3). Clay and fine silt concentrations increase abruptly at the boundary between Unit II and III (Fig. 2c). Average sand contents do not differ significantly from Unit II, but certain samples, for example, from 10.25, 5.25 and 1.25 cm, exhibit exceptionally low sand concentrations < 5% while clay and fine silt concentration peak at the same time (Figs 2c–d). Al, Ti and Zr concentrations as well as Fe/S ratios are generally high (Fig. 5). BSi, TOC*, TN and P concentrations increase towards the sediment surface, while B and Ca concentrations deviate from this trend in the upper 5 cm (Figs 4b and 6). A strong increase in the Fe/S ratio is visible in the uppermost 4 cm (Fig. 5d). TOC/TN ratios of Unit III are the lowest of the record (Fig. 4a) with an average of 10.5.

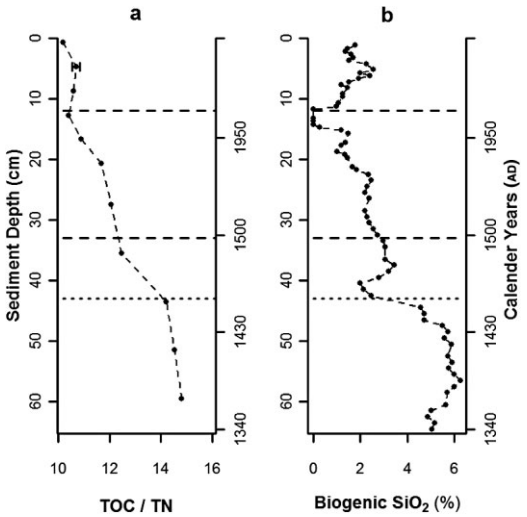

Fig. 4. Molar TOC/TN ratios and biogenic SiO_2 (BSi) concentrations: (a) High molar TOC/TN ratios point to higher percentages of organic matter derived from macrophytes. (b) BSi concentrations are assumed to be governed by the burial of diatom frustules. Note the distinct change in both records between 44 and 35 cm sediment depth (~AD 1450 and AD 1490). Horizontal dashed lines show the borders of units and subunits.

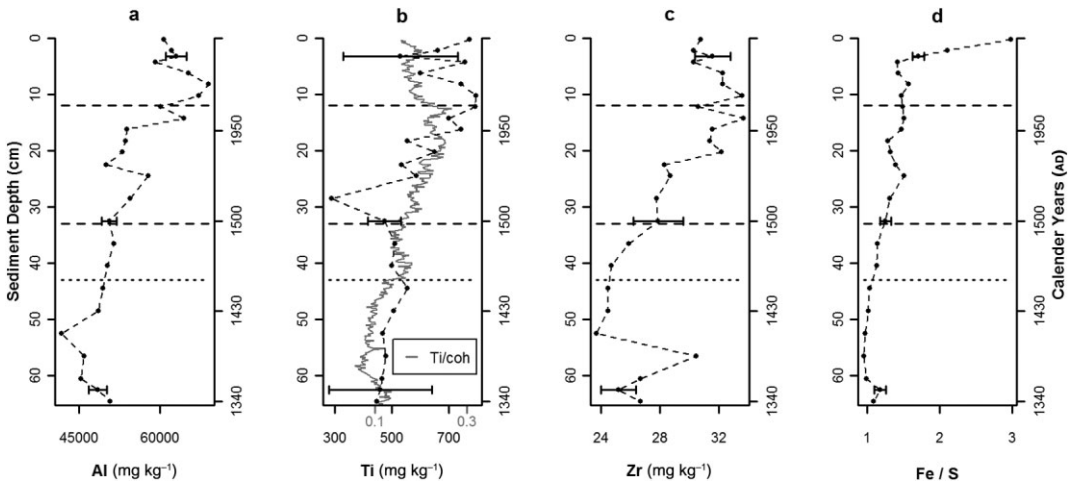

Fig. 5. Indicators for minerogenic sediment input: (a) Al, (b) Ti and (c) Zr (Group 1 elements) and (d) Fe/S ratios. Data obtained from XRF scans (Ti/coh) confirm Ti concentrations determined by ICP-OES that show comparatively large error bars. Fe/S ratios are mainly governed by the degree of pyritization and minerogenic sediment input. High Fe/S ratios above 3 cm sediment depth point to the presence of a redoxcline. Horizontal dashed lines show the borders of units and subunits.

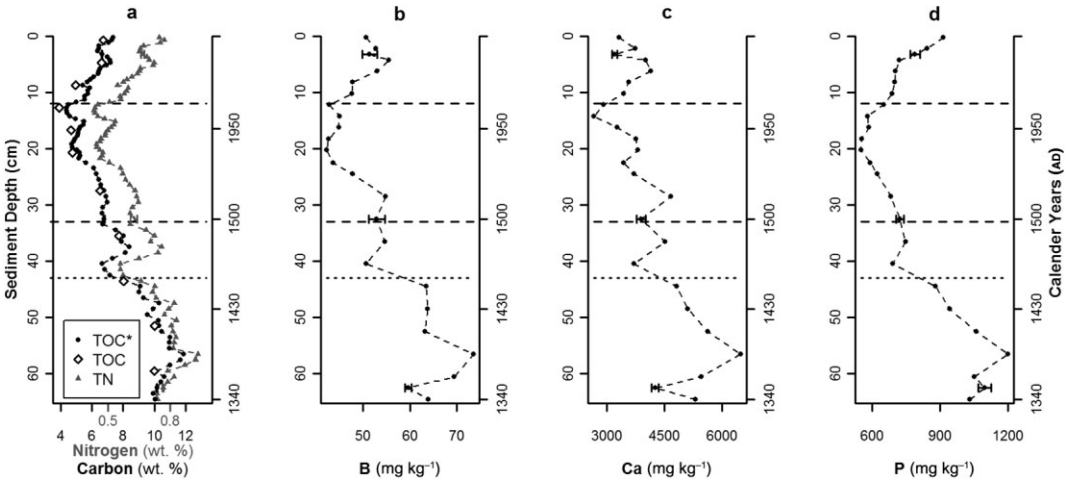

Fig. 6. Concentrations of elements mainly attributable to autochthonous sediment production and marine influences (Group 2 elements): (a) total carbon (TOC*), total organic carbon (TOC) and total nitrogen (TN), (b) B, (c) Ca and (d) P. Note the parity between total carbon (TOC*) and total organic carbon (TOC) concentrations. Horizontal dashed lines show the borders of units and subunits.

Table 3. Percentages of grain size fractions and mean grain size in Units I, II and III of EV 10.1. Concentrations of coarse sand (630–2000 µm) are zero in all samples.

		Clay < 2 µm (%)	Fine silt < 6.3 µm (%)	Medium silt < 20 µm (%)	Coarse silt < 63 µm (%)	Fine sand < 200 µm (%)	Medium sand < 630 µm (%)	Mean grain size (µm)
Unit III	Mean	21	27	26	17	9	< 1	7.5
(0–12 cm)	Min	17	23	24	15	2	0	5.7
	Max	24	34	29	20	13	1	9.1
Unit II	Mean	18	22	30	20	9	< 1	8.8
(12–33 cm)	Min	12	20	27	18	6	0	7.1
	Max	22	24	36	23	13	1	10.4
Unit I	Mean	17	20	27	24	11	1	10.5
(33–65 cm)	Min	15	16	22	19	8	0	8.5
	Max	21	26	31	28	14	6	14.0

Linking proxies and processes

Indicators for allochthonous and autochthonous sediment origin

Correlation between element concentrations does not necessarily imply a common origin for those elements but is likely to indicate similar variations of burial flux under certain environmental conditions. A correlation scheme exhibits two main groups of elements whose concentrations show similar trends throughout the record (Fig. 7). Almost all elements can be ascribed to one of the groups, if an inter-element correlation coefficient threshold of $R = 0.5$ is used.

Group 1 includes elements often used as indicators for allochthonous minerogenic input into lakes such as Al, Ti and Zr (Boës *et al*. 2011), which are applicable here considering the predominance of batholithic and metamorphic rocks in the catchment (Potgieter 1949). The high correlation between Al and K ($R = 0.69$; $p < 0.001$) and Ba and K ($R = 0.80$; $p < 0.001$) suggests a prevalent detrital origin, possibly from feldspars and clay minerals. Group 2 comprises elements such as TOC*, TN, Ca, Sr, P, B and BSi which are highly correlated ($R > 0.8$; $p < 0.001$) to each other. Strong correlations between Ca, Mg and Sr in sediments of the Wilderness Lakes were already found by Watling (1977), but TIC concentrations not exceeding 0.6 wt. % in any sample of the record point to rather low carbonate contents. Very strong correlations between P and

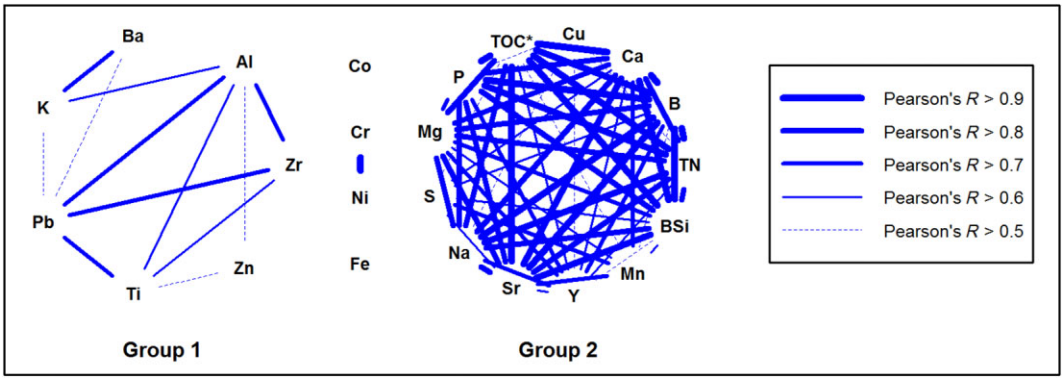

Fig. 7. Correlation scheme of element concentrations. Pearson's product-moment correlation was used. With the exception of Fe, Ni, Co and Cu, all elements can be either ascribed to Group 1 (containing indicators for minerogenic sediment input) or Group 2 (containing indicators for autochthonous sediment formation and/or marine influences).

TOC* ($R = 0.94$; $p << 0.001$) and TN ($R = 0.92$; $p << 0.001$) suggest P burial flux to be primarily controlled by the accumulation and decomposition of organic matter which is consistent with findings from Howard-Williams (1980). BSi contents are probably governed by the deposition of diatom frustules and may therefore be interpreted as a proxy for phytoplankton production. The correlation between TOC* and BSi concentrations is notable ($R = 0.96$; $p << 0.001$). The transfer of B from saline waters into sediment is a process typically found in the saline–freshwater mixing zone of estuarine systems (Park and Schlesinger 2002). Thus, many Group 2 elements are indicative for marine influences and autochthonous sediment production. Elements such as Mn, S, Cu or Fe, Ni, Co and Cr exhibit weaker correlations (Fig. 7) and represent elements that are typically subject to processes associated with early diagenesis or redox reactions leading to the mobilization of certain element species in the sediment (Boyle 2001).

Fe/S ratios governed by pyrite formation as indicator for minerogenic input

Fe/S ratios in the core are governed by pyrite (FeS_2) formation, a microbial-mediated process typically found in coastal environments where adequate amounts of sulphates, reactive Fe (= HCl or dithionite extractable Fe fraction; Raiswell *et al*. 1994) and metabolizable organic matter are available (Morse *et al*. 2007). A TOC*-Fe-S ternary plot (Fig. 8a) shows that Fe/S ratios follow the stoichiometric pyrite line (Fe/S = 0.8702 by mass). XRD measurements confirm the presence of pyrite in all examined samples, although only traces were found in the sample from 0.75 cm (data not shown). The correlation of Fe and S concentrations is highest in Subunit Ia, being characterized by high TOC* contents (65–43 cm; $R = 0.83$, $p << 0.001$), and still significant ($R = 0.74$, $p < 0.01$) in the other sections of the core. The decline of S concentrations from 2.3% to 0.9% points to a redoxcline in the uppermost 3 cm (Fig. 8b) and a predominantly diagenetic pyrite formation (Holmer and Storkholm 2001). The two near-surface samples (0–3 cm) can be identified as outliers in the ternary plot (Fig. 8a). Due to marine influences pyrite formation is not limited by the availability of S (Morse *et al*. 2007), whereas Fe content in the sediment is controlled by both pyrite formation and the supply of Fe from the catchment (Watling 1977). This is underscored by the high correlation ($R = 0.84$; $p << 0.001$) between Fe/Al ratios and S concentrations (Figs 8b, c). The presence of non-pyrite Fe species can be deduced from the Fe surplus compared with the pyrite line in all samples (Fig. 8c). Under the simplifying assumption that S is entirely bound in pyrite, non-pyrite Fe contents (= total Fe – $0.8702 \times$ S by mass) correlate highly significantly with Al concentrations ($R = 0.81$; $p << 0.001$). Therefore, Fe/S ratios, being less sensitive to depletion effects than element concentrations, can be used as independent proxies for minerogenic input.

TOC/TN ratios as indicator for the origin of accumulated organic matter

TOC/TN ratios provide information on the origin of buried organic substances. Molar ratios in organic matter originating from phytoplankton normally range in value between 4 and 10, whereas

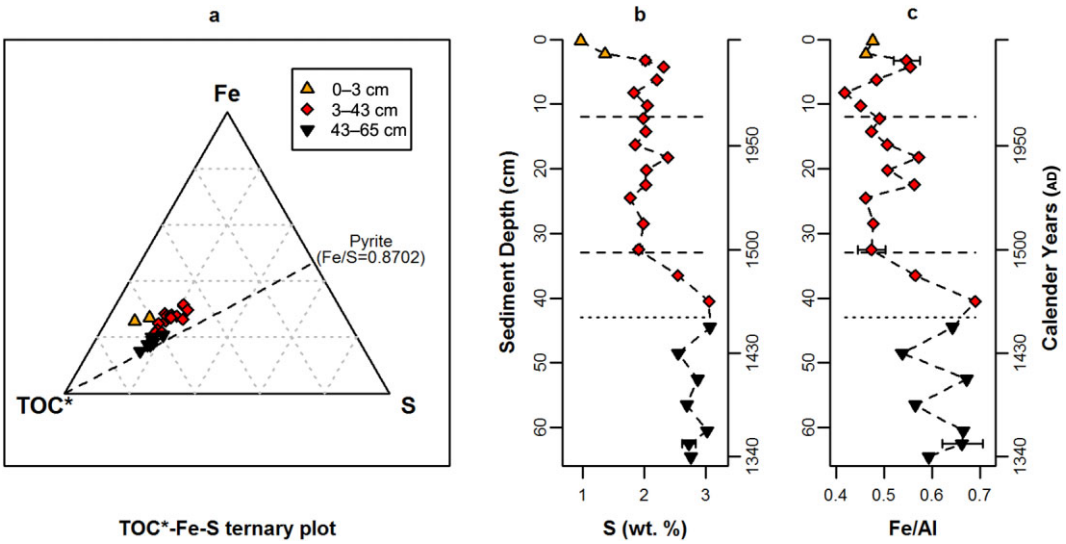

Fig. 8. Relationships between Fe, S and TOC*: (a) The TOC*-Fe-S ternary plot shows that Fe/S ratios in EV 10.1 follow the stoichiometric pyrite line, especially below 43 cm sediment depth (prior to ~AD 1450) where highest TOC* concentrations were found. The two uppermost samples are identifiable as outliers attributable to a decline of (b) S concentrations and point to a redoxcline below 3 cm sediment depth. S concentrations correlate with (c) Fe/Al mass ratios (normalization with Al was used to account for variable Fe input from the catchment). Horizontal dashed lines show the borders of units and subunits.

vascular plants containing cellulose are characterized by values > 20 (Meyers and Teranes 2001; Mayr *et al*. 2005). In EV 10.1 ratios range between 10 and 15 and suggest a mixed signal of phytoplankton and vascular plants. Some caution regarding the interpretation of TOC/TN ratios is warranted for deposits of the last century, since TN loss normally exceeds TOC loss after the very initial decay of unstable organic compounds (Gälman *et al*. 2008).

Grain size distributions as indicator for erosion, transport and accumulation processes

Grain size composition reflects the intensity and spatial heterogeneity of erosion as well as transport processes and selective accumulation. Sand is present across most of the catchment due to widespread sand sheets and weathering products of granite and sandstone (Illenberger 1996). Dune areas next to Eilandvlei contain 28% fine sand and > 98% sand in total (Bateman *et al*. 2011). The closest source area of sand, Eilandvlei's island, is ~160 m from the coring site and largely covered by dense vegetation. Even during high wind speed transport in suspension is restricted to particles < 150 µm (Tsoar and Pye 1987), leading to the conclusion that sand content is a poor indicator for aeolian transport. Instead, wave cut erosion and subsequent transport by currents in addition to flood events contribute to the supply of sand (Marker 2004). The main sources for fine sediment (< 6.3 µm, clay and fine silt) in the catchment are weathered topsoils and alluvium stored along flow paths and in wetlands. Grain size-dependent fractionation of sediment during transport proceeds within the lake (Birch *et al*. 1978). In shallow waters, especially away from macrophyte stands, wave-induced resuspension of sediment and subsequent deposition in deeper lake areas is to be expected (Woszczyk *et al*. 2011). Therefore, it can be hypothesized that mean grain size and sand content decrease with rising water level and consequently increasing distance to coarser sediments next to the shoreline. In addition, decreasing mean grain size can result from changing sediment provenance, increasing fine sediment flux from the catchment and changes in trap efficiency in either the catchment or the lake.

Discussion

Environmental change pre-dating the arrival of European colonists

Sedimentation at the coring site is characterized by steadily increasing concentrations of fine minero-

genic sediment components starting around AD 1450 (Fig. 5) and therefore ~375 years prior to the onset of colonial land-use along the Wilderness Coast (Phillips 1931). Assuming hunter-gatherers had a minimal impact on the environment, changes in sediment dynamics prior to the arrival of European colonists were most likely caused by climate and/or sea level fluctuations (Baxter and Meadows 1999).

The relative sea-level rise at the Knysna Estuary, 35 km west of Eilandvlei (Fig. 1a), may have amounted to as much as 0.7–2 m since ~AD 1300 (Marker 1997). Based on changes of the facies distribution in the Langebaan Lagoon (Fig. 1a), Compton (2001) suggested a ~0.5 m lower sea level than present in ~AD 1250. Past sea-level rise would likely have increased the mean lake level of Eilandvlei, since it is mainly controlled by the water level of the Touw River Estuary. Additionally, sea-level rise would be likely accompanied by a rising groundwater table. An increasing distance of the coring position to the shoreline due to rising lake levels can explain reduced sedimentation rates and the deposition of finer sediments at the coring site after ~AD 1500. Table 4 indicates that, in comparison to Unit I (~AD 1330–1490), burial flux rates of Group 1 elements as well as burial flux rates of Group 2 elements were reduced during the deposition of Unit II (~AD 1490–post AD 1950). Increasing Al, Ti and Zr concentrations in Unit II (Figs 5a–c) can be attributed to a disproportional decline of burial flux rates of elements, indicating marine influences and/or autochthonous sediment production.

In addition, climate variations, i.e. the *Little Ice Age* (*LIA*), may have altered sediment dynamics in the Wilderness Lakes region. According to Tyson *et al*. (2000), the LIA (~AD 1300–1800) was the most pronounced climate anomaly in southern Africa since the Mid-Holocene. The $\delta^{18}O$ record from the Cango Caves indicates a 1–2°C lower mean annual temperature during this period (Talma and Vogel 1992). Chase and Meadows (2007) suggested that the influence of the westerlies was accentuated in cool phases while monsoonal systems weakened. Therefore, higher proportions of winter rainfall and reduced precipitation in austral summer months are to be expected. Changes in the precipitation–evaporation balance during the LIA may have directly influenced erosion rates and sediment transport in the catchment of Eilandvlei and potentially affected its lake level in periods of a closed Touw River Estuary mouth. Similar to this study, Stager *et al*. (2012) found an increasing sediment delivery to Verlorenvlei, Western Cape, starting about AD 1400, which was suggested to be the consequence of LIA climate variations.

Furthermore, the amount and seasonal distribution of rainfall has important implications for the regional vegetation. Wet spells in the Holocene promoted the expansion of afrotemperate forests, whereas during drier periods fynbos vegetation spread out onto marginal forest sites (Martin 1968; Geldenhuys 1994); the most recent forest expansion cycle probably started between AD 0 and 1000 (Martin 1968; Scholtz 1986). In contrast, trees in less favourable habitats might have been susceptible to drought stress in summer months during the LIA

Table 4. Mean burial flux rates (mg cm^{-2} yr^{-1}) of selected elements in Units I, II and III of EV 10.1 and ratios between Unit III and Unit I. Best estimates correspond to sedimentation rates derived from the Clam algorithm (based on median ages). Minimum and maximum values were calculated using minimum and maximum sedimentation rate estimates, respectively.

		Group 1 elements			Group 2 elements			
		Al	Ti	Zr	Ca	P	B	TOC*
Unit III	Best	44 000	490	22	2500	520	35	44 100
(0–12 cm)	Min	40 000	450	20	2300	470	32	40 200
	Max	50 000	560	25	2900	590	40	50 300
Unit II	Best	7000	70	4	800	140	9	7500
(12–33 cm)	Min	6000	60	3	600	120	8	6300
	Max	9000	100	5	1000	180	12	9800
Unit I	Best	20 000	200	11	2100	390	26	33 900
(33–65 cm)	Min	10 000	110	6	1100	200	14	17 500
	Max	84 000	870	46	9000	1670	110	143 000
Unit III/Unit I	Best	2.2	2.4	2.0	1.2	1.3	1.3	1.3
	Min	0.47	0.52	0.43	0.26	0.28	0.28	0.28
	Max	4.8	5.3	4.4	2.6	2.9	2.9	2.9

and it is conceivable that an increase of veld and forest fires occurred. Based on palynological investigations on fen deposits from Groenvlei, 20 km east of Eilandvlei (Fig. 1a), Martin (1968) inferred a forest decline predating colonial times. Unfortunately, actual timing of the forest decline is vague (Martin 1968) and another pollen stratigraphy from the Wilderness region with a comparable temporal resolution is currently not available.

Ecological change in Eilandvlei pre-dating the arrival of European colonists

The decline of TOC/TN ratios between ~AD 1440 and AD 1490 (44–35 cm) indicates a changing significance of sources providing organic matter. This is most likely associated with ecological change within Eilandvlei considering the simultaneous decline of BSi and TOC* concentrations (Figs 4 and 6). A likely explanation is an increased occurrence of submerged macrophytes closer to the coring position prior to ~AD 1450 (Meyers and Teranes 2001; Haberzettl *et al*. 2005), for example, due to lower water turbidity or a lower lake level. Higher burial flux of organic matter from macrophyte stands may have fostered the diagenetic fixation of sulphur in pyrite (Fig. 8c).

Cyclic changes in the distribution of submerged macrophytes have been observed in all Wilderness Lakes during the past decades (see Weisser *et al*. 1992) and various causes have been discussed, including fungal diseases, shading effects of algal blooms, changes in water salinity and fish stock or waterfowl biomass (Russell *et al*. 2009). Reduced light availability due to the intrusion of turbid water during flood events was also argued to be a limiting factor for the occurrence of subaquatic macrophytes (Howard-Williams 1980). It is possible, that the dark layers in the radiography (43–39 cm; Fig. 2a) and the comparatively high amount of sand in Subunit Ib (~AD 1450–1490; Fig. 2d) bears witness to high-energy flood events initiating ecological change in Eilandvlei. In contrast to recent observations, the ecological shift that is reflected in TOC* and BSi concentrations as well as TOC/TN ratios was apparently unidirectional for several centuries (Figs 4 and 6a). Therefore, we assume that changing environmental conditions during the LIA and/or sea-level rise triggered long-term changes in the lake system. Investigations of the diatom assemblage being already undertaken (Kirsten unpubl.) will likely help to elucidate cause and effect relationships.

Increasing human impact since the late nineteenth or early twentieth century

The impact of land-use change on sediment dynamics following the arrival of European colonists has been previously demonstrated at several sites along the Cape coast (e.g. Baxter and Meadows 1999; Marker 2004; Neumann *et al*. 2010). The colonization of the Wilderness Embayment by woodcutters started in the second half of the eighteenth century (Phillips 1931). This period unfortunately corresponds to a section in the sedimentary record that is characterized by a low temporal resolution. However, in its early stages, the selective exploitation of wood resources preferentially took place in easily accessible forests. Large-scale exploitation of the area did not occur until AD 1882 (Phillips 1931).

The sedimentary record of Eilandvlei indicates that deforestation amplified sediment mobilization. The age-depth model (Fig. 3) points to distinctive increases in mean sedimentation rates after AD 1950 (from 16.5 cm). Due to the discrete distribution of dated samples it is possible that elevated sediment input started several decades earlier. Pastoral and agricultural land-use could have increased the flux of Al, Ti, Zr, P and N into the lake. In particular, the catchment of the Duiwe River is presently heavily cultivated and has previously been identified as a source area for suspended solids and nutrients (Allanson and Whitfield 1983; Russell 2013). Additional supply of dissolved nutrients was possibly delivered from the sea due to frequent artificial opening of the Touw River Estuary and reduced river runoff because of water abstraction for irrigation and domestic use. A subsequent increase of biomass production in Eilandvlei may be reflected in the decline of TOC/TN ratios starting after AD 1840 (Fig. 4a). Ongoing diagenetic processes may still increase TOC/TN ratios in the upper parts of the sediment sequence (Gälman *et al*. 2008), which needs to be addressed, when interpreting the record. However, algal blooms and short-term eutrophic conditions were frequently observed in Wilderness Lakes during the past decades and are likely a consequence of human impact (Russell 2003). Although dating uncertainties leave room for interpretation, a comparison of mean burial flux rates between Unit I and III indicates a twofold increase in minerogenic sediment input, whereas autochthonous sediment production seems to increase by only 25% (Table 4).

A doubling of minerogenic sediment input, that is, soil erosion rates only twice as high as precolonial erosion rates, is very moderate in comparison to other South African sites (e.g. Compton *et al*. 2010). However, sediment from 33% of the watershed, including areas from which high sediment yields can be expected, that is, the slopes of the Outeniqua Mountains and cultivated land, is now partially stored behind small farm dams (Fig. 1b). The considerable impacts of small reservoirs on sediment flux have been previously demonstrated (Boardman and Foster 2011; Baade *et al*. 2012). We hypothesize that the distinct increase in clay and fine silt percentages after AD 1950 (above 12 cm; Fig. 2c) reflects the construction of farm dams against the background of ongoing accelerated soil erosion. Coarse silt and sand are more effectively trapped in reservoirs than fine sediment (Verstraeten and Poesen 2000), which might explain high clay and fine silt percentages in Unit III. Peaks of clay and fine silt associated with exceptionally low sand content in the uppermost 11 cm of the core (Figs 2c–d) probably refer to flood events during the last decades, when highly turbid water entered Eilandvlei (Allanson and Whitfield 1983).

Conclusions

The synopsis of granulometric and geochemical data from the sediment record EV 10.1 indicates that sediment dynamics along the Wilderness Embayment changed markedly during the past ~670 years. Concentrations of minerogenic sediment components started to increase around AD 1400 and thus ~375 years prior to the advent of European colonists. This can be attributed to LIA climate variations that altered the amount and seasonal distribution of rainfall. Reduced summer rainfall during the LIA possibly triggered a recession of afrotemperate forests and affected runoff patterns, sediment mobilization and transport in the catchment. A rising mean lake level, for example, as a consequence of sea-level rise or an altered water balance, offers an additional explanation for the observed changes in the record. A contemporaneous ecological change in Eilandvlei is indicated by decreasing TOC/TN ratios and decreasing burial flux of BSi and TOC*. Future studies of diatom, pollen and charcoal assemblages will help to disentangle the effects of climate variations and sea-level change during the LIA period.

Increasing mean sedimentation rates towards more recent times are consistent with previous observations and are attributable to human interference. Higher concentrations of minerogenic sediment components point to accelerated soil erosion in the catchment since the late nineteenth or early twentieth century following the conversion of natural vegetation to agricultural and forestry land. It is suggested that increasing nutrient flux (e.g. TN and P) from the catchment in the second half of the twentieth century contributed to rising autochthonous biomass production. A comparison of mean burial flux rates of elements between the fourteenth/fifteenth century and the past decades point to an increase in autochthonous sediment production by 25% and a twofold increase in minerogenic sediment input into the lake. As numerous farm ponds act as sinks along the sediment transport path, the latter magnitude most probably underestimates changes in catchment erosion.

Acknowledgements

Financial support from the International Bureau, Bundesministerium für Bildung und Forschung (BMBF, Germany, grant SUA 09/10), the National Research Foundation (NRF, South Africa, grant UID 72083) and participating universities as well as logistic support from SANParks Scientific Services, Rondevlei, is gratefully acknowledged. B. Dreßler, C. Kirchner and K. Hartwig conducted laboratory analysis. S. Clausnitzer compiled data for the bathymetric map. M. Ahlborn and S. Truckenbrodt are thanked for fruitful discussions. Gauge data were kindly provided by the Department of Water Affairs and Forestry (DWAF), George, South Africa; the Department of Environmental Affairs (DEA), South Africa, provided access to the CSIR Special Report FIS 147. I.D.L. Foster and an anonymous reviewer are acknowledged for constructive comments on an earlier version of the manuscript.

Bastian Reinwarth, Sarah Franz, Jussi Baade, Torsten Haberzettl, Thomas Kapser, Gerhard Daut and Roland Mäusbacher
Physische Geographie, Institut für Geographie, Friedrich-Schiller-Universität Jena, Löbdergraben 32, 07743 Jena, Germany
Email: bastian.reinwarth@uni-jena.de

Jörg Helmschrot
Biozentrum Klein Flottbek und Botanischer Garten, Biodiversität, Evolution und Ökologie der Pflanzen (BEE), Universität Hamburg, Ohnhorststr. 18, 22609 Hamburg, Germany
Email: joerg.helmschrot@uni-hamburg.de

Kelly L. Kirsten, Lynne J. Quick and Michael E. Meadows
Department of Environmental and Geographical Science, University of Cape Town, Private Bag X3, Rondebosch 7701, South Africa
Email: mmeadows@mweb.co.za

References

Ad-Hoc AG Boden (Ad-Hoc-Arbeitsgruppe der Staatlichen Geologischen Dienste und der Bundesanstalt für Geowissenschaften und Rohstoffe), 2005. *Bodenkundliche Kartieranleitung. 5th ed*. Schweizerbart, Stuttgart, 438 p.

Allanson, B.R. and Whitfield, A.K., 1983. *The Limnology of the Touw River Floodplain*. South African National Scientific Programmes Report, 79. CSIR, Pretoria, 35 p.

Baade, J., Franz, S. and Reichel, A., 2012. Reservoir siltation and sediment yield in the Kruger National Park, South Africa: a first assessment. *Land Degradation & Development*, 23 (6), 586–600. doi: 10.1002/ldr.2173

Bateman, M.D., Carr, A.S., Dunajko, A.C., Holmes, P.J., Roberts, D.L., McLaren, S.J., Bryant, R.G., Marker, M.E. and Murray-Wallace, C.V., 2011. The evolution of coastal barrier systems: a case study of the Middle-Late Pleistocene Wilderness barriers, South Africa. *Quaternary Science Reviews*, 30, 63–81. doi: 10.1016/j.quascirev.2010.10.003

Baxter, A.J. and Meadows, M.E., 1999. Evidence for Holocene sea level change at Verlorenvlei, Western cape, South Africa. *Quaternary International*, 56, 65–79. doi: 10.1016/S1040-6182(98)00019-6

Birch, G.F., du Plessis, A. and Willis, J.P., 1978. Offshore and onland geological and geophysical investigations in the Wilderness Lakes region. *Transactions of the Geological Society of South Africa*, 81, 339–352.

Blaauw, M., 2010. Methods and code for 'classical' age-modelling of radiocarbon sequences. *Quaternary Geochronology*, 5 (5), 512–518. doi: 10.1016/j.quageo.2010.01.002

Blott, S.J. and Pye, K., 2001. Gradistat: a grain size distribution and statistics package for the analysis of unconsolidated sediments. *Earth Surface Processes and Landforms*, 26, 1237–1248. doi: 10.1002/esp.261

Boardman, J. and Foster, I.D.L., 2011. The potential significance of the breaching of small farm dams in the Sneeuberg region, South Africa. *Journal of Soils and Sediments*, 11 (8), 1456–1465. doi: 10.1007/s11368-011-0425-5

Boës, X., Rydberg, J., Martinez-Cortzas, Bindler, R. and Renberg, I., 2011. Evaluation of conservative lithogenic elements (Ti, Zr, Al, and Rb) to study anthropogenic element enrichments in lake sediments. *Journal of Paleolimnology*, 46 (1), 75–87. doi: 10.1007/s10933-011-9515-z

Boyle, J.F., 2001. Inorganic geochemical methods in paleolimnology. In: Last, W.M. and Smol, J.P. (eds), *Tracking Environmental Change Using Lake Sediments. Volume 2: Physical and Geochemical Methods*. Kluwer Academic Publishers, Dordrecht. 83–141.

Chase, B.M. and Meadows, M.E., 2007. Late Quaternary dynamics of southern Africa's winter rainfall zone. *Earth-Science Reviews*, 84, 103–138. doi: 10.1016/j.earscirev.2007.06.002

Coetzee, D.J., 1983. Zooplankton and environmental conditions in a southern Cape coastal lake system. *Journal of the Limnological Society of Southern Africa*, 9 (1), 1–11. doi: 10.1080/03779688.1983.9639405

Compton, J.S., 2001. Holocene sea-level fluctuations inferred from the evolution of depositional environments of the southern Langebaan Lagoon salt marsh, South Africa. *The Holocene*, 11 (4), 395–405. doi: 10.1191/095968301678302832

Compton, J.S., Herbert, C.T., Hoffman, M.T., Schneider, R.R. and Stuut, J.-B., 2010. A tenfold increase in the Orange River mean Holocene mud flux: implications for soil erosion in South Africa. *The Holocene*, 20 (1), 115–122. doi: 10.1177/0959683609348860

Dearing, J.A., 1999. *Environmental Magnetic Susceptibility. Using the Bartington MS2 System. 2nd ed*. Chi Publishing, Kenilworth, UK. 54 p.

DeMaster, D.J., 1980. The half life of ^{32}Si determined from a varved Gulf of California sediment core. *Earth and Planetary Science Letters*, 48 (1), 209–217. doi: 10.1016/0012-821X(80)90182-X

Dewar, G., Reimer, P.J., Sealy, J. and Woodborne, S., 2012. Late-Holocene marine radiocarbon reservoir (ΔR) for the west coast of South Africa. *The Holocene*, 22 (12), 1481–1489. doi: 10.1177/0959683612449755

DIN (Deutsches Institut für Normung), 2008. *DIN 32645:2008-11. Chemische Analytik – Nachweis-, Erfassungs- und Bestimmungsgrenze. Ermittlung unter Wiederholbedingungen. Begriffe, Verfahren, Auswertung*. Beuth, Berlin. 29 p.

Gälman, V., Rydberg, J., Sjöstedt de-Luna, S., Bindler, R. and Renberg, I., 2008. Carbon and nitrogen loss rates during aging of lake sediment: Changes over 27 years studied in varved lake sediment. *Limnology and Oceanography*, 53 (3), 1076–1082. doi: 10.4319/lo.2008.53.3.1076

Geldenhuys, C.J., 1994. Bergwind fires and the location pattern of forest patches in the southern Cape landscape, South Africa. *Journal of Biogeography*, 21 (1), 49–62. doi: 10.2307/2845603

Gordon, N., García-Rodríguez, F. and Adams, J.B., 2012. Paleolimnology of a coastal lake on the Southern Cape coast of South Africa: sediment geochemistry and diatom distribution. *Journal of African Earth Sciences*, 75, 14–24. doi: 10.1016/j.jafrearsci.2012.06.008

Grimm, E.C., 1987. CONISS: a FORTRAN 77 program for stratigraphically constrained cluster analysis by the method of incremental sum of squares. *Computers & Geosciences*, 13 (1), 13–35. doi: 10.1016/0098-3004(87)90022-7

Haberzettl, T., Fey, M., Lücke, A., Maidana, N., Mayr, C., Ohlendorf, C., Schäbitz, F., Schleser, G.H., Wille, M. and Zolitschka, B., 2005. Climatically induced lake level changes during the last two millennia as reflected in sediments of Lake Potrok Aike, southern Patagonia (Santa Cruz, Argentina). *Journal of Paleolimnology*, 33, 283–302. doi: 10.1007/s10933-004-5331-z

Holmer, M. and Storkholm, P., 2001. Sulphate reduction and sulphur cycling in lake sediments: a review. *Freshwater Biology*, 46 (4), 431–451. doi: 10.1046/j.1365-2427.2001-00687.x

Howard-Williams, C., 1980. Aquatic macrophyte communities of the Wilderness Lakes: community structure and

associated environmental conditions. *Journal of the Limnological Society of Southern Africa*, 6 (2), 85–92. doi: 10.1080/03779688.1980.9634551

Illenberger, W.K., 1996. The geomorphologic evolution of the Wilderness dune cordons. *Quaternary International*, 33, 11–20. doi: 10.1016/1040-6182(95)00099-2

Jarvis, A., Reuter, H.I., Nelson, A. and Guevara, E., 2008. *Hole-filled SRTM for the globe Version 4,* available from the CGIAR-CSI SRTM 90m database: http://srtm.csi.cgiar.org (file: srtm_41_19.tif) (11-Jun-11).

Kasper, T., Haberzettl, T., Doberschütz, S., Daut, G., Wang, J., Zhu, L., Nowaczyk, N. and Mäusbacher, R., 2012. Indian Ocean Summer Monsoon (IOSM)-dynamics within the past 4 ka recorded in the sediments of Lake Nam Co, central Tibetan Plateau (China). *Quaternary Science Reviews*, 39, 73–85. doi: 10.1016/j.quascirev.2012.02.011

Kelts, K., Briegel, U., Ghilardi, K. and Hsu, K., 1986. The limnogeology-ETH coring system. *Swiss Journal of Hydrology*, 48 (1), 104–115. doi: 10.1007/BF02544119

Klein, R.G., 1983. Paleoenvironmental implications of Quaternary large mammals in the fynbos region. In: Deacon, H.J., Hendey, Q.B. and Lambrechts, J.J.N. (eds), *Fynbos paleoecology: a preliminary synthesis*. South African National Programmes Report No. 75. CSIR, Pretoria. 116–138.

Manning, M.R. and Melhuish, W.H., 1994. Atmospheric $\delta^{14}CO_2$ record from Wellington. In: Boden, T.A., Kaiser, D.P., Sepanski, R.J. and Stoss, F.W. (eds), *Trends: a compendium of data on global change*. Carbon Dioxide Information Analysis Center, Oak Ridge National Laboratory, Oak Ridge. 173–202.

Marker, M.E., 1997. Evidence for a Holocene low sea level at Knysna. *South African Geographical Journal*, 79 (2), 106–107. doi: 10.1080/03736245.1997.9713631

Marker, M.E., 2004. Changes in the Salt River, tributary to the Knysna Estuary, South Africa: 1936–1998. *South African Geographical Journal*, 86 (2), 131–140. doi: 10.1080/03736245.2004.9713817

Martin, A.R.H., 1959. The stratigraphy and history of Groenvlei, a South African coastal fen. *Australian Journal of Botany*, 7 (2), 142–167. doi: 10.1071/BT9590142

Martin, A.R.H., 1968. Pollen analysis of Groenvlei lake sediments, Knysna (South Africa). *Review of Paleobotany and Palynology*, 7, 107–144. doi: 10.1016/0034-6667(68)90029-8

Mayr, C., Fey, M., Haberzettl, T., Janssen, S., Lücke, A., Maidana, N.I., Ohlendorf, C., Schäbitz, F., Schleser, G.H., Struck, U., Wille, M. and Zolitschka, B., 2005. Palaeoenvironmental changes in southern Patagonia during the last millennium recorded in lake sediments from Laguna Azul (Argentina). *Palaeogeography, Palaeoclimatology, Palaeoecology*, 228, 203–227. doi: 10.1016/j.palaeo.2005.06.001

McCormac, F.G., Hoog, A.G., Blackwell, P.G., Buck, C.E., Higham, T.F.G. and Reimer, P.J., 2004. SHCal04 Southern Hemisphere Calibration, 0–11.0 cal kyr BP. *Radiocarbon*, 46 (3), 1087–1092.

Meyers, P.A. and Teranes, J.L., 2001. Sediment organic matter. In: Last, W.M. and Smol, J.P. (eds.), *Tracking Environmental Change Using Lake Sediments. Volume 2: Physical and Geochemical Methods*. Kluwer Academic Publishers, Dordrecht, 239–269.

Morse, J.W., Thomson, H. and Finneran, D.W., 2007. Factors controlling sulfide geochemistry in sub-tropical estuarine and bay sediments. *Aquatic Geochemistry*, 13, 143–156. doi: 10.1007/s10498-007-9012-1

Neumann, F.H., Scott, L., Bousman, C.B. and van As, L., 2010. A Holocene sequence of vegetation change at Lake Eteza, coastal KwaZulu-Natal, South Africa. *Review of Palaeobotany and Palynology*, 162 (1), 39–53. doi: 10.1016/j.revpalbo.2010.05.001

Ohlendorf, C. and Sturm, M., 2008. A modified method for biogenic silica determination. *Journal of Paleolimnology*, 39, 137–142. doi: 10.1007/s10933-007-9100-7

Park, H. and Schlesinger, W.H., 2002. Global biochemical cycle of boron. *Global Biochemical Cycles*, 16 (4), 20.1–20.11. doi: 10.1029/2001GB001766

Phillips, J.F.V., 1931. *Forest-Succession and Ecology in the Knysna Region*. *The Government Printer. Pretoria.* 327 p.

Potgieter, C.T., 1949. *The structure and petrology of the George granite plutons and invaded pre-Cape sedimentary rocks*. PhD diss. University of Stellenbosch, Stellenbosch, South Africa.

Raiswell, R., Canfield, D.E. and Berner, R.A., 1994. A comparison of iron extraction methods for the determination of degree of pyritisation and the recognition of iron-limited pyrite formation. *Chemical Geology*, 111, 101–110. doi: 10.1016/0009-2541(94)90084-1

Reimer, P.J., Brown, T.A. and Reimer, R.W., 2004. Discussion: reporting and calibration of post-bomb ^{14}C data. *Radiocarbon*, 46 (3), 1299–1304.

Russell, I.A., 2003. Changes in the distribution of emergent aquatic plants in a brackish South African estuarine-lake system. *African Journal of Aquatic Science*, 28 (2), 103–122. doi: 10.2989/16085910309503776

Russell, I.A., 2013. Spatio-temporal variability of surface water quality parameters in a South African estuarine lake system. *African Journal of Aquatic Science*, 38 (1), 53–66. doi: 10.2989/16085914.2012.742006

Russell, I.A., Randall, R.M., Randall, B.M. and Hanekom, N., 2009. Relationships between the biomass of waterfowl and submerged macrophytes in a South African estuarine lake system. *Ostrich: Journal of African Ornithology*, 80 (1), 35–41. doi: 10.2989/OSTRICH.2009.80.1.5.763

Schneider, H., Höfer, D., Trog, C., Busch, S., Schneider, M., Baade, J., Daut, G. and Mäusbacher, R., 2010. Holocene estuary development in the Algarve Region (Southern Portugal) – a reconstruction of sedimentological and ecological evolution. *Quaternary International* 221, 141–158. doi: 10.1016/j.quaint.2009.10.004

Scholtz, A., 1986. *Palynological and palaeobotanical studies in the southern Cape*. MA diss. University of Stellenbosch, Stellenbosch, South Africa.

Scott, L. and Lee-Thorp, J.A., 2004. Holocene climatic trends and rhythms in southern Africa. In: Battarbee, R.W., Gasse, F. and Stickley, C.E. (eds), *Past Climate Variability through Europe and Africa*. Springer, Dordrecht. 69–91.

Sealy, J., Ludwig, B. and Henderson, Z., 2006. New radiocarbon dates for Matjes River rock shelter. *The South African Archaeological Bulletin*, 61 (183), 98–101.

Stager, J.C., Mayewski, P.A., White, J. Chase, B.M., Neumann, F.H., Meadows, M.E., King, C.D. and Dixon, D.A., 2012. Precipitation variability in the winter rainfall zone of South Africa during the last 1400 yr linked to the austral westerlies. *Climate of the Past*, 8 (3), 877–887. doi: 10.5194/cp-8-877-2012

Talma, A.S. and Vogel, J.C., 1992. Late Quaternary paleotemperatures derived from a speleothem from Cango Caves, Cape Province, South Africa. *Quaternary Research*, 37 (2), 203–213. doi: 10.1016/0033-5894(92)90082-T

Tsoar, H. and Pye, K., 1987. Dust transport and the question of desert loess formation. *Sedimentology*, 34, 139–153. doi: 10.1111/j.1365-3091.1987.tb.00566.x

Tyson, P.D., Karlén, W., Holmgren, K. and Heiss, G.A., 2000. The Little Ice Age and medieval warming in South Africa. *South African Journal of Science*, 96, 121–126.

Verstraeten, G. and Poesen, J., 2000. Estimating trap efficiency of small reservoirs and ponds: methods and implications for the assessment of sediment yield. *Progress in Physical Geography*, 24 (2), 219–251. doi: 10.1177/030913330002400204

Watling, R.J., 1977. *Trace metal distribution in the wilderness lakes*. National Physical Research Laboratory. Special Report FIS 147. CSIR, Pretoria. 73 p.

Weisser, P.J., Whitfield, A.K. and Hall, C.M., 1992. The recovery and dynamics of submerged aquatic macrophyte vegetation in the Wilderness lakes, southern Cape. *Bothalia*, 22 (2), 283–288.

Woszczyk, M., Bechtel, A. and Cieśliński, R., 2011. Interactions between microbial degradation of sedimentary organic matter and lake hydrodynamics in shallow water bodies: insights from Lake Sarbsko (northern Poland). *Journal of Limnology*, 70 (2), 293–304. doi: 10.3274/JL11-70-2-09

Xu, B., Yang, X., Gu, Z., Zhang, Y., Chen, Y. and Lv, Y., 2009. The trend and extent of heavy metal accumulation over last one hundred years in the Liaodong Bay, China. *Chemosphere*, 75 (4), 442–446. doi: 10.1016/j.chemosphere.2008.12.067

Manuscript received 4 Jan., 2013, revised and accepted 17 May, 2013